

The Use of a Large-strain Drying and Consolidation Model to Optimise Multilift Tailing Deposits

P J Vardon¹, Y Yao², L A van Paassen³ and A F van Tol^{4,5}

ABSTRACT

Thin-lift atmospheric fine drying (AFD) is a technique used to dewater mine and oil sand tailings, which utilises both self-weight consolidation and atmospheric evaporation. The disposed layers undergo a cyclic drying and rewetting process due to precipitation and deposition of additional lifts on top of the dried layer. The current research aims to optimise the deposition process via use of a numerical model and realistic atmospheric conditions, including both periods of drying and wetting. The model is based upon water balance and includes large strain considerations. A number of material behaviours are characterised using empirical fitting curves based upon laboratory measurement of material characteristics, including both the shrinkage and water retention curves for drying and rewetting. The model is able to model multiple lifts, simulating field scale and realistic climatic conditions within timescales suitable for engineering practice (eg seconds or minutes). The model has been previously validated against controlled laboratory experiments and utilised to simulate field tests. A series of simulations are presented to illustrate the ability of the model to be used as a practical tool for the optimisation of a tailings deposition strategy.

INTRODUCTION

Treatment of fine grained tailings is a major challenge in the mining industry. Such materials are produced in the order of millions of tonnes per year globally, with large amounts already stored (Wang *et al*, 2014). In general, fine grained tailings are a mixture of clay and silt particles suspended in water, which remains after mining extraction. Due their small grain size, these particles settle very slowly from the liquid suspension, segregating them from coarser particles. Settling can be accelerated by adding flocculants, but even after settling, these materials often retain much more water than a lot water, resulting in a high water content and low consistency. These tailings are usually stored in large tailings ponds and, without additional measures, can take decades for the fine particles to dewater, therefore causing significant challenges in the amount of land that is required and long-term legacy costs. One technology to treat these tailings which is currently being evaluated is atmospheric fines drying (AFD) (Shell, 2012). In this technology, fine grained tailings are mixed with a flocculant to help the particles settle and increase the speed of dewatering. The material is then laid in layers in a drying area which is open to the atmosphere, installed with a surface slope to actively drain water that has been driven out of the material or rain run-off. The fluid fines after flocculation quickly form a two phase material, where separate fluid pressures and inter-granular stresses exist. At

this point consolidation behaviour occurs due to both self-weight consolidation and evaporation. Large changes in the water content leads to large differences in permeability, drainage lengths and compressibility not usually characterised in consolidation models. Moreover, unsaturated behaviour and soil-atmosphere interaction is often not well represented.

This paper first presents a model developed to characterise this atmospheric drying behaviour. The model follows on from developments reported by van der Meulen *et al* (2012), Nijssen (2013) and Vardon *et al* (2014) where the model was initially validated against laboratory data and includes permeability, stiffness, and drainage length changes within a single phase model. The model implementation is described, with a number of features designed to allow models to be solved within reasonable timescales for design purposes. The model behaviour is presented in an idealised numerical case study to demonstrate how the model could be utilised in design. Details of the computational performance are also presented.

THEORETICAL FORMULATION

The theoretical basis of the model has previously been reported (Kim, Diels and Feyen, 1992, implemented by van der Meulen *et al*, 2012; Nijssen, 2013) and therefore is only briefly reported here for clarity, alongside the implementation

1. Assistant Professor, Geo-Engineering Section, Delft University of Technology, PO Box 5048, 2600 GA Delft, The Netherlands. Email: p.j.vardon@tudelft.nl
2. PhD student, Geo-Engineering Section, Delft University of Technology, PO Box 5048, 2600 GA Delft, The Netherlands. Email: y.yao@tudelft.nl
3. Assistant Professor, Geo-Engineering Section, Delft University of Technology, PO Box 5048, 2600 GA Delft, The Netherlands. Email: l.a.vanpaassen@tudelft.nl
4. Professor, Geo-Engineering Section, Delft University of Technology, PO Box 5048, 2600 GA Delft, The Netherlands. Email: a.f.vantol@tudelft.nl
5. Scientific Board Member, Deltares, PO Box 177, 2600 MH, Delft, The Netherlands.

details. The main approach of the model is to consider the mass conservation of the water, considers the volumetric water content as the primary variable to be solved, and focus is made on the water flow behaviour. The mechanical (stress-strain) parts of the model are incorporated via material property relationships.

Other models simulating similar processes have been previously presented. Seneviratne *et al* (1996) presented the MinTaCo model, which, makes the pore-water pressure the primary variable and solves using the finite element method. This work utilises only the air-entry value to control behaviour in the unsaturated flow zone. Yao and Znidarcic (1997) produced the CONDESO model which solves saturated flow below a desiccation limit and a separate desiccation theory above this limit. Boundary conditions are set only as a constant velocity or surcharge. Stark, Choi and Schroeder (2005) present a model focusing on the settlement of such material, with the deformation as the primary variable, with an admittedly simplistic approach for the evaporative drying.

In this paper, the processes in drying/wetting behaviour in tailings ponds are reduced to a 1D scenario, considering the lateral extent is normally large with respect to the vertical. As the soil undergoes large deformations, a material level coordinate system has been adopted:

$$dm = \frac{dz}{1+e} \quad (1)$$

where:

- m is the 1D material coordinate
- z is the Cartesian (real) coordinate
- e is the void ratio

Water transport

Water transport is governed by Darcy's Law with the water potential, ϕ , made up from a gravimetric component, z , an overburden component (the excess pore pressure in head), Ω , and a suction component, φ .

The conservation of mass yields:

$$\frac{\partial \Theta}{\partial t} = \frac{\partial^2}{\partial z^2} [K(\varphi + z + \Omega)] \quad (2)$$

where:

- Θ is the volumetric water content $\Theta = V_w/V_t$
- V_w and V_t are the volume of water and total volume
- t is time
- K is the hydraulic conductivity

The overburden component of the water potential is determined via Equation 3, with use of the change of void ratio with change in water ratio to govern the proportion of the overburden taken by the pore water:

$$\Omega = \frac{\partial e}{\partial \theta} \int_{z_0}^z \gamma dz \quad (3)$$

where:

- e is the void ratio
- z is the depth
- z_0 is the depth at the surface
- γ is the volumetric weight

By substitution of z for m by Equation 1, $\Theta = \theta/(1+e)$, $K^* = K/(1+e)$, $\gamma = \frac{\theta + \gamma_s}{1+e}$, the chain rule for differentials, and integration by parts yields the final governing equation:

$$\frac{\partial \theta}{\partial t} = \frac{\partial}{\partial m} \left\{ K^* \left[\frac{\partial \varphi}{\partial \theta} \cdot \frac{\partial \theta}{\partial m} + (1+e) + (\theta + \gamma_s) \frac{\partial \varphi}{\partial \theta} + \frac{\partial^2 e}{\partial \theta^2} \int_{z_0}^z (\theta + \gamma_s) dm \cdot \frac{\partial \theta}{\partial m} \right] \right\} \quad (4)$$

Equation 4 must then be solved in time and space, with the other variables material parameters. The suction is linked to the volumetric water ratio, $\theta = V_w/V_s$ (where V_w and V_s are the volumes of water and solids), via an empirically determined soil water retention curve (SWRC). It is worth noting that the SWRC cannot, in the case of such a material with large deformations, be linked only to degree of saturation as the material may remain saturation over a large range of volumetric water contents. Both the well-known van Genuchten SWRC and the modified van Genuchten SWRC (Romero and Vanaut, 2000) have been implemented. The modified van Genuchten curve limits the maximum suction predicted by the SWRC which aids computational efficiency, eliminating extreme non-linearity in very dry areas. As this model is designed for virgin soils (sludges) subsequent re-wetting re-drying loop is likely to be significantly different from the first drying behaviour, with a lower water content yielded for the same suction value. Therefore, following the approach of Rijniersce (1983), a ten times stiffer relationship in a log-linear space has been utilised, which leads to a reduced swelling with rewetting matching observed behaviour, although due to a lack of experimental evidence has not been included as a separate parameter here.

The hydraulic conductivity, K , used is a function of void ratio and degree of saturation. The (saturated) hydraulic conductivity of the system, K , is related to the water content by a log-linear relation (Kim, Diels and Feyen, 1992) and fitted to available data:

$$K_{sat} = 10^{A_{HCC}\theta - B_{HCC}} \quad (5)$$

where:

A_{HCC} and B_{HCC} are material parameters determined from experimental data

The unsaturated hydraulic conductivity is governed by two Equations 6 and 7, the first, governs the reduction in hydraulic conductivity with saturation and the second the increased hydraulic conductivity with desiccation cracks:

$$K_{rel} = S_l^{\delta} \quad (6)$$

$$K_{dess} = 1 \text{ if } h-z > d_{dess} \\ K_{dess} = (1 - \epsilon_{dess}) + \epsilon_{dess} \exp(\xi_{dess}(1 - S_l)) \text{ if } h-z < d_{dess} \quad (7)$$

where:

- S_l is the degree of saturation
- δ is a material parameter and is related to the pore size distribution
- z is the same as the gravitational potential (positive upwards), in this case with the zero datum at the base of the sludge
- h is the total height of the sludge column
- d_{dess} is the depth from the surface where desiccation and other surface effects act

ϵ_{dess} and ξ_{dess} are material parameters.

The final hydraulic conductivity is the product of Equations 5, 6 and 7.

The drying/wetting processes considered at the atmospheric boundary, are:

Base boundary:

1. open (fixed zero potential), or
2. closed (natural no flow boundary condition).

Top (atmospheric) boundary:

1. Flux boundary condition, calculated using the maximum of the average evaporation potential (including precipitation and the inverse) and the soil flux in the last element, ie the water movement due to consolidation or evaporation. Any free water is assumed to run-off.

The top boundary has been set up so that a time series of evaporation potentials/precipitation can be input.

Soil deformation

The soil deformation is governed by a shrinkage curve – an empirical material curve linking the volumetric water content, $\theta = V_w/V_s$ (where V_w and V_s are the volumes of water and solids), and the void ratio. Hysteretic re-swelling behaviour and non-linear compression due to additional overburden are also included. The shrinkage curve is defined as (Fredlund, Wilson and Fredlund, 2002):

$$e = A_{sh} \left(\frac{\theta^{C_{sh}}}{B_{sh}^{C_{sh}}} + 1 \right)^{\frac{1}{C_{sh}}} \quad (8)$$

where:

- A_{sh} is the minimum void ratio
- B_{sh} is a parameter defining the slope
- C_{sh} is a parameter defining the transition between the linear portion and the minimum void ratio

The degree of saturation at which the sludge initially dries from is defined as B_{sh} / A_{sh} . Parameter A_{sh} is defined as a function of overburden stress as:

$$A_{sh} = A_{sh}^0 \left[1 - \frac{1}{C_{10}} \log \left(\frac{\sigma'}{\sigma'_0} \right) \right] \quad (9)$$

where:

- A_{sh}^0 is defined as the minimum void ratio under zero overburden conditions
- σ' is the current stress
- σ'_0 is the initial stress
- C_{10} is a material parameter

In addition, re-wetting behaviour has been shown to be hysteretic, therefore a separate re-wetting curve has been included as:

$$e = v_h - b(\theta - \xi_h)^2 \text{ where } b = \frac{v_h - v_z}{\xi_h^2} \quad (10)$$

where:

- v_h is void ratio at the maximum swelling
- ξ_h is the water content at the maximum swelling
- v_z is the minimum void ratio of the previous shrinkage phase

Both Equations 8 and 10 are illustrated in Figure 1. In subsequent drying curves, B_{sh} is redefined at the current position and Equation 8 again utilised.

Soils gain strength with compression, and therefore liability for fluid fine tailings may be reduced. This may be characterised and easily included as an output to the model or via post-processing of the model results.

IMPLEMENTATION

The theoretical formulation has been implemented in a discrete spatial domain via a finite difference formulation, and solved recognising the highly non-linear behaviour utilising an explicit Runge-Kutta method as implemented in Matlab. The domain is discretised into equally sized finite difference cells within each layer, with material properties evaluated at the cell centre, and fluxes evaluated at the cell boundaries. To account for hysteresis behaviour a constant time delay, ie not based upon the timestep, has been incorporated, via the selection of the dde23 solver (Shampine and Thompson, 2001).

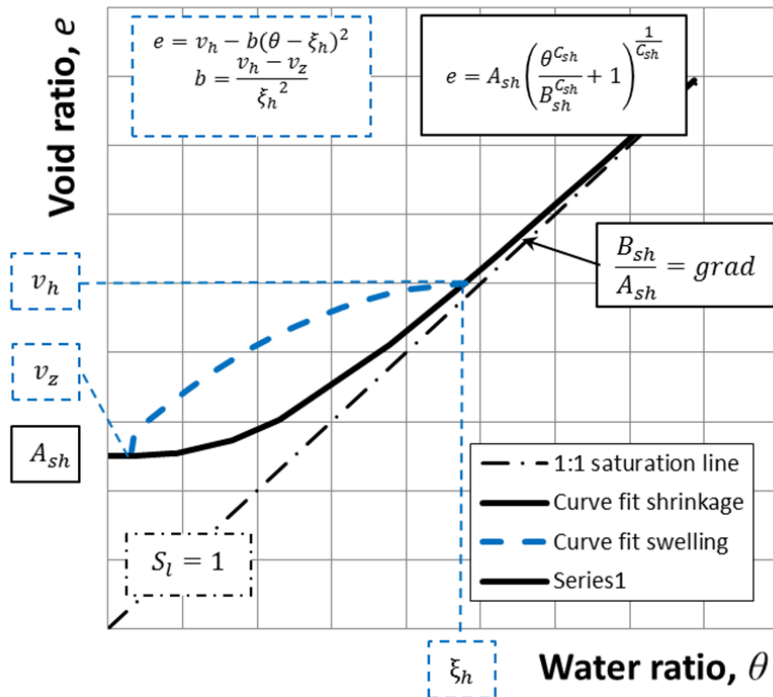


FIG 1 – Shrinkage curve including re-wetting hysteretic behaviour.

This ensures that a consistent evaluation of hysteretic behaviour can be undertaken.

A user interface has been developed utilising the Matlab interface, so that the model can be easily operated. A main graphical window, controls the analysis, with separate windows for inputting:

- the material properties
- the simulation settings (eg number of material layers, atmospheric conditions, etc)
- plotting the results.

The simulations are able to be saved, loaded or run from the main window. A suite of data files is used to contain the analysis data (geometry, precipitation conditions), the material data and the results. Figure 2, shows an overview of the user interface.

CASE STUDY

A case study has been implemented to investigate the model performance. It is assumed that settlement has finished and consolidation begins at deposition. In this case study 10 m (original) depth of fine tailings is deposited in differing strategies. In a 100 m × 100 m disposal pond, this equates to 100 000 m³ of fluid fine tailings. The tailings are deposited over a two-year period, and left for a further two years. A number of different potential strategies are simulated as shown in Table 1. The tailings are considered to have an initial water ratio of 3.5 (equal to a gravimetric water content of 152 per cent or 40 per cent wt solid content) and simulations have been started at the beginning of a winter period. The model has been discretised into 10 cm layers.

TABLE 1
Simulated deposition strategies.

Name	Number of layers	Depth (m)	Deposition (days)
Single stack	1	10	0
Thick stack	4	2.5	0 then every 182.5
Thin stack	10	1	0 then every 73
Thick winter – thin summer stack	6	3 (2 No.) and 1 (4 No.)	0 then every 122
Thin winter – thick summer	6	1 (4 No.) and 3 (2 No.)	0 then every 122
Thick stack winter only	4	2.5	0 then every 365

Material properties

The material properties selected in this paper are idealised and not based on a particular fluid fine. However, they have been selected to be representative of a fluid fine composed of silty-clay material.

The solid volumetric weight of $\gamma_s = 23 \text{ kN/m}^3$ has been used and the shrinkage curve parameters from Equation 8 are $A_{sh}^0 = B_{sh} = 0.48$, $C_{sh} = 4.5$ and additionally $C_{10} = 10$ from Equation 9 with an initial stress of 1 kPa defined. Rewetting behaviour defined by Equation 10 has been defined by the following parameters: $v_{hi} = \xi_{hi} = 1$.

The modified van Genuchten equation has been used in this case study:



FIG 2 – Overview of the user interface: (A) is the main controller to load other windows, run simulation, save results and load analyses, (B) is the simulation settings window; (C) is the material properties window, and (D) plots the results.

$$S_e = C(s) \left(\frac{1}{(1 + (\alpha_{WRC} \cdot \phi)^{n_{WRC}})^{m_{WRC}}} \right)$$

$$C(s) = 1 - \left(\frac{\ln \left[1 + \frac{\phi}{\alpha_{WRC}} \right]}{\ln(2)} \right) \quad (11)$$

$$S_e = \frac{\theta - WCR}{WCS - WCR}$$

where:

S_e is the effective degree of saturation
 WCR is the residual (volumetric) water content
 WCS is the water content at full saturation

α_{WRC} , n_{WRC} , m_{WRC} and ϕ are fitting parameters
 m_{WRC} is defined as $m_{WRC} = 1 - 1 / n_{WRC}$

In this work, $WCR = 0.2$, $WCS = 2.2$, $\alpha = 50\,000$ cm, $\alpha_{WRC} = 0.11$ cm and $n_{WRC} = 1.23$. This is shown in Figure 3. It is noted that in this model, this relationship controls final deformations as well, and the suction against void ratio plot (Figure 3) can be considered as vertical effective stress against void ratio.

Equation 5, defining the saturated hydraulic conductivity, has been utilised with $A_{HCC} = 1.6$ and $B_{HCC} = 4.4$ and is presented in Figure 4; $\delta = 3$ in Equation 6 and Equation 7 has not been used in this case study.

Atmospheric conditions (idealised)

The atmospheric conditions simulated have been distilled into a net mean precipitation or evaporation, with the precipitation positive sign convention. Monthly values have been used, which are deemed to be reasonable as slopes to aid run-off are shallow and run-off would not be immediate. This assumption is linked to management and climatic conditions, eg the extent to which a one day (or one hour) storm would run off, or locally pool is not considered here. A climatic condition with a moisture deficit (ie the integral of the net mean precipitation/evaporation curve is negative), as it is in these climatic regions where atmospheric drying would be utilised. A two-year idealised climatic condition is shown in Figure 5 and this condition is repeated to give four years' data. The first year in the two-year series has an overall dryer

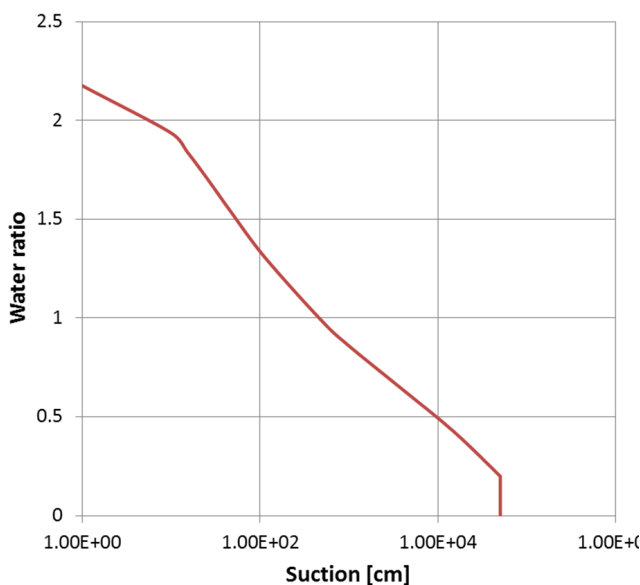


FIG 3 – Soil water retention curve used in the analyses.

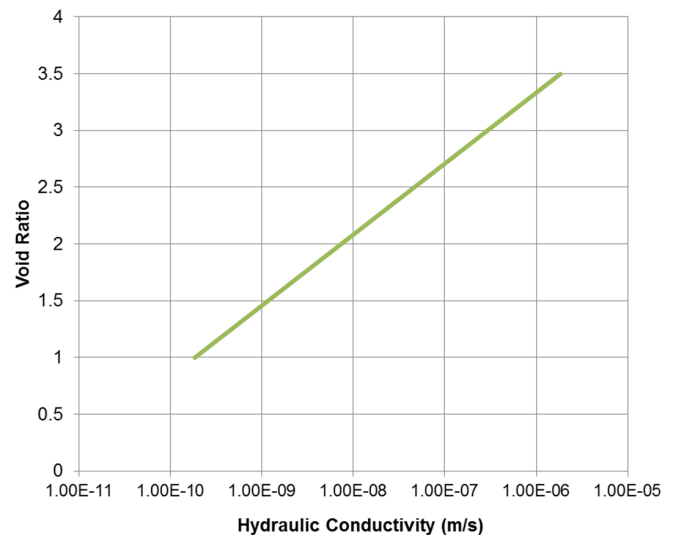


FIG 4 – Saturated hydraulic conductivity variation with void ratio.

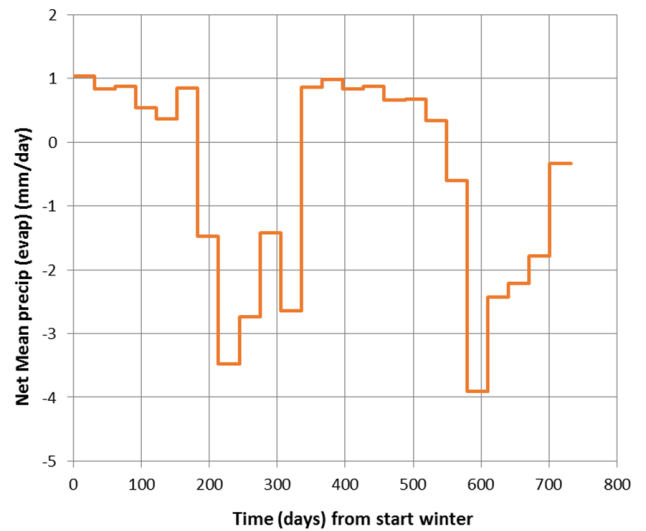


FIG 5 – Climatic data modelled.

summer, but the second year has a more intense, but shorter, dry period.

For the base boundary condition, both open and closed cases have been simulated, but as in all cases the soil becomes more dense at the base and the hydraulic conductivity reduces, there is little overall difference. In the results presented, closed base drainage has been set.

RESULTS

The results from the case study are presented below. Table 2 summarises the depth at two, three and four years, from an original total depth of deposition of 10 m. It can be seen that for all of the scenarios the reduction in initial height is 38–45 per cent of the original height. The difference in total height between the first five scenarios is not significant, although by examining both the void ratio and water fluxes some significant differences can be observed. The 'Single stack' and 'Thick stack' analyses will be presented in more detail and examined.

Figure 6a shows the settlement of the layers against time for the 'Single stack' analysis whereas Figure 6b shows the same for the 'Thick stack' analysis; Figure 7 presents the water fluxes of the same analyses; and Figure 8 shows void ratio profiles. For Figure 8 the material level coordinates given in Equation 1

TABLE 2

Depth at two years, three years and four years after the start of deposition.

Name	Depth (m) at 2 years	Depth (m) at 3 years	Depth (m) at 4 years
Single stack	6.64	6.56	6.15
Thick stack	6.74	6.31	6.04
Thin stack	6.71	6.29	6.02
Thick winter – thin summer stack	6.61	6.26	5.99
Thin winter – thick summer	6.70	6.19	5.93
Thick stack winter only	2.74/5.24 (2/3 layers)	4.08/6.58 (3/4 layers)	5.46

are utilised to aid comparison. In Figure 6a a generally smooth settlement can be seen, decreasing over time. There is one major increase in gradient between approximately 600–700 days, which coincides with the second summer, and highlights the lack of such a feature in the third summer, with again an increase in gradient in the fourth. In Figure 7a the initial positive flux (water leaving the material) is derived by the overburden potential; this is the typical result from consolidation analysis. At between 200 and 300 days a small increase in flux is noted – which is due to the evaporation of the first summer. However, the level of flux is comparable in magnitude and therefore does not contribute significantly to the settlement. There is a large increase in flux, approximately three times for the second summer, with also almost no increase in flux for the third summer and another increase

at the fourth summer. Figure 8a shows that for the void ratio profiles a relatively deep dense crust is formed due to evaporation after the first year. This zone has a low hydraulic conductivity and therefore restricts further flow from below and from the atmosphere. This crust re-wets from both upwards and downwards flow over the next year and again allows evaporation in the fourth summer, from re-saturating desaturated parts and from allowing some swelling.

In Figure 6b, the four deposited layers can be easily seen. In each new layer a smooth settlement curve occurs, with a number of periods of increased drying due to evaporation, located in the last two summers. Figure 7b, highlights this, with additional fluxes due to evaporation also apparent in the other summers, but at the same magnitude as the overburden driven flux. In Figure 8b two layers can be easily seen, in contrast with the four layers that were deposited. These show that the layering is only well defined when the evaporative flux causes over consolidation of the layer. The first layer shows a crust of decreased void ratio (more dense) but this crust is rather limited in depth, leading to the only limited benefit in additional settlement and associated strength gains. This layer also has an effect of sealing the below layers as it has a low hydraulic conductivity. Comparing Figures 8a and 8b also shows that the ‘crust’ (the surface layer), is thicker for the ‘Thick stack’ which would suggest a higher surface bearing capacity.

All of the analyses with more lifts showed only limited impact of the additional drying, as they all miss a portion of the times when evaporation is possible and therefore no significant differences are noted. There are all better than

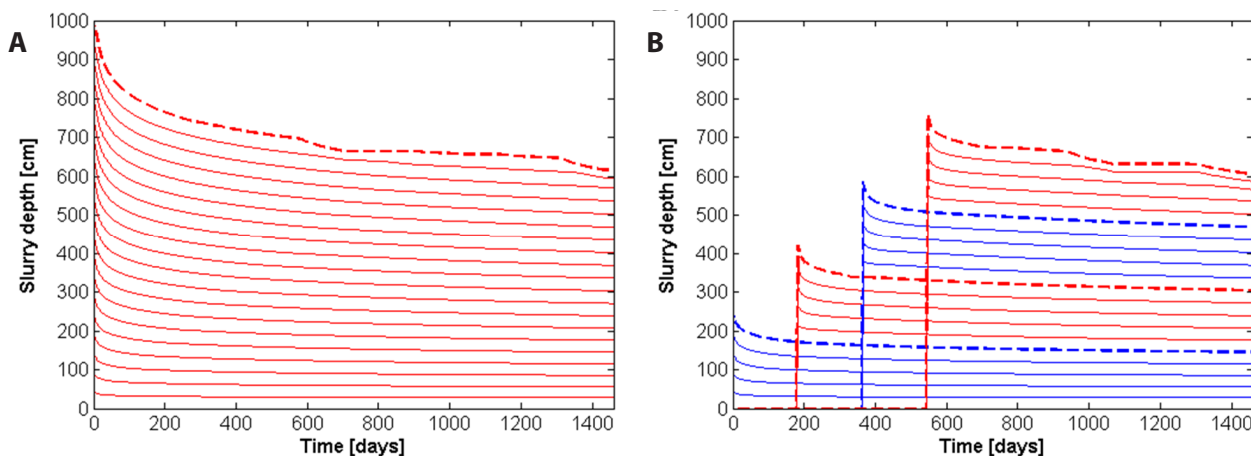


FIG 6 – Settlements against time for the (A) ‘Single stack’ and (B) ‘Thick stack’ analyses.

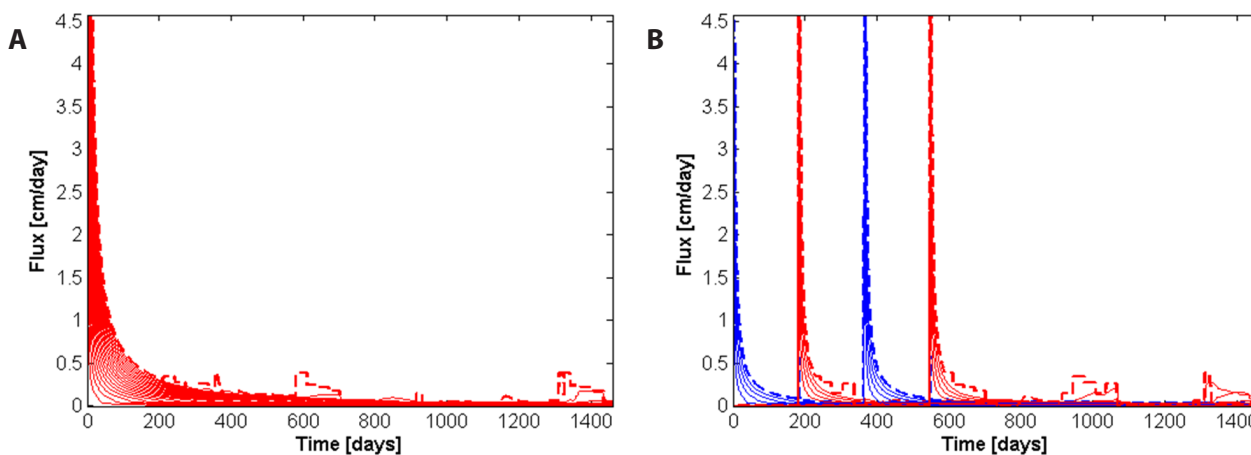


FIG 7 – Water fluxes against time for the (A) ‘Single stack’ and (B) ‘Thick stack’ analyses.

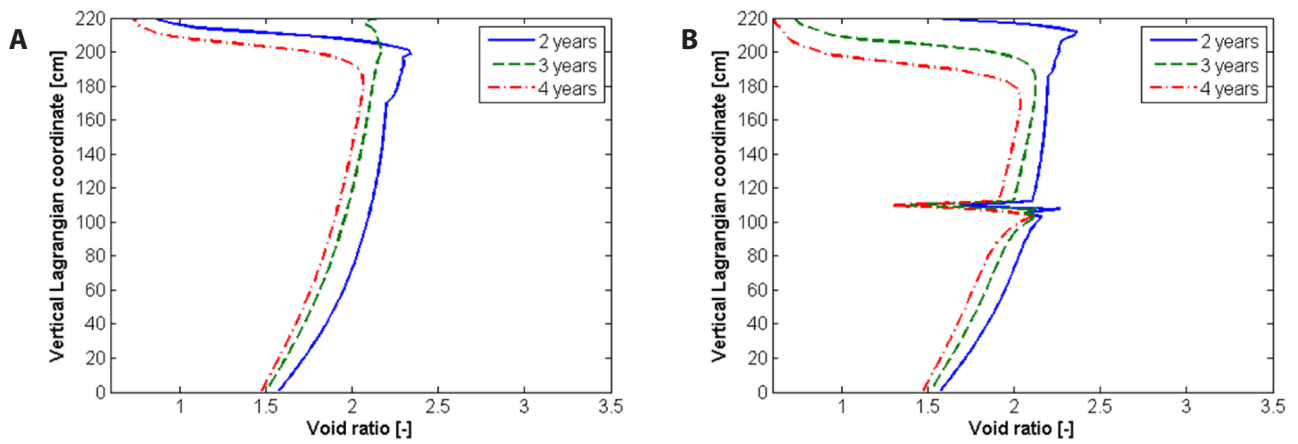


FIG 8 – Void ratio profiles at two, three and four years the (A) ‘Single stack’ and (B) ‘Thick stack’ analyses.

the single lift however, as the water has a smaller distance to travel through the recently deposited layers, so the initial self-weight consolidation is faster. It is worth noting that further consolidation for the deep layers will be very slow as the deep unsaturated crust provides a hydraulic barrier to further flow. This means that for deep layers, if self-weight consolidation is sufficient, it may be better to ensure that the top surfaces remain wet (saturated) and do not form an low permeability crust, and for thinner layers to ensure that a period of evaporation occurs. The exact tuning of the system is likely to be based upon regulation or risk/liability assessments for particular materials.

The sixth analysis makes an attempt to tune the behaviour to take into account both the self-weight consolidation and the evaporative fluxes. In this analysis 2.5 m layers are deposited in the winter and allowed to consolidate under self-weight (overburden). Figure 9a shows the void ratio profiles and Figure 9b the water fluxes. Table 2 gives the settlement, which is ~50 cm (or five per cent of total original height) more than other analyses. What is seen in Figure 9a is that all layers are distinct and have a portion with low void ratio (high density) and from Figure 9b each summer period has a distinct period of evaporative flux. In the summer, the evaporative fluxes are significantly higher than the self-weight consolidation and therefore drive the water loss. This causes each layer to be significantly further consolidated and will, after later water redistribution, produce a more homogenous, denser material.

For all the cases examined the majority of the deformation occurs due to self-weight consolidation. The fluxes in high water content fluid fines, due to self-weight consolidation, are likely to be initially higher than those possible from

evaporation. This highlights the importance of well-designed run-off and drainage and supports the practice of underwater consolidation, which does not allow a low permeability crust to form. However, additional consolidation, and therefore settlements and additional strength, may be yielded from evaporative fluxes. For these to have significant impact, periods of evaporative fluxes must last enough time for water to move from a reasonable depth. It should be noted that the dynamics of the analyses for different materials depend on their material properties.

If regulation or risk/liability assessments require a strength over that of simply normally-consolidated materials then evaporative drying can yield such materials. If the deposition can be tuned in such a way so that self-weight consolidation takes place when evaporation potential is low, ie during the winter half of the year, then evaporation potential can be used to further consolidate prior to the next deposition. This means that the layer thickness should be calibrated to enable self-weight consolidation to be to a high percentage complete, and so that the required depth of the layer can be further reduced in water content over the summer half of the year. Water redistribution within these layers can then take place over longer periods of time, leading to a more homogenous material, but one that is over-consolidated and therefore stronger. This is in agreement with the concept of Optimised Seasonal Deposition presented by Caldwell *et al* (2014) who propose placing three different depths of flocculated fine tailings at different times of the year to benefit most from climatic conditions and achieve required strengths.

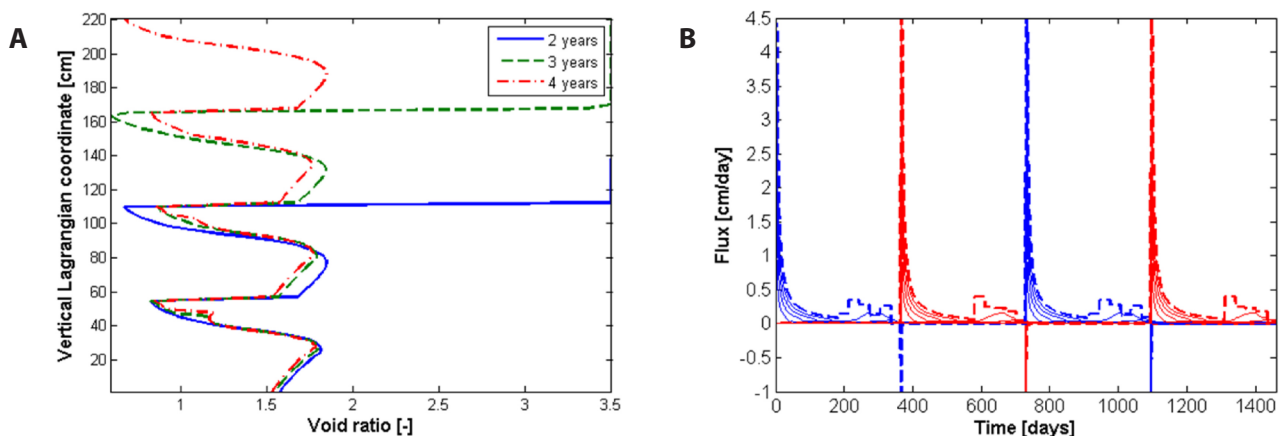


FIG 9 – Void ratio profiles and water fluxes against time for the ‘Thick stack winter only’ analysis.

COMPUTATIONAL PERFORMANCE

The total computational time has been measured for the analyses as an indication of whether the model could be easily incorporated into engineering practice. The computer that the models have been executed on is a Dell Precision T3500, with a six-core 3.47 GHz Intel Xeon (W3690) process and 12 GB RAM. This model has been implemented in Matlab serially, ie only to use one core, but all models can be therefore run simultaneously if memory does not restrict performance. In this case the models utilise approximately 200 MB of memory.

Table 3 indicates the performance times. In all cases the same domain discretisation has been utilised, ie 10 cm cells. The non-linearity of the material behaviour, leads to differences in the solutions and in the main, increases, where larger depths have unsaturated behaviour and large gradients due to new layers on already desaturated layers. It is noted that all times are relatively low, and this indicates that such a model could be easily integrated into engineering practice.

TABLE 3
Time taken for four-year simulations.

Name	Time of execution (mins:secs)
Single stack	14:58
Thick stack	12:41
Thin stack	12:57
Thick winter – thin summer stack	14:15
Thin winter – thick summer	14:27
Thick stack winter only	14:43

CONCLUSIONS

A model simulating the consolidation behaviour of fluid fines has been developed which includes both self-weight consolidation and evaporation driven consolidation. The model is designed to be suitable for materials with initially high water contents, and therefore updates geometry and hydraulic conductivity in response to large deformations. The model also includes unsaturated flow and the response of the soil to unsaturated conditions. Hysteretic behaviour in the swelling and shrinkage, and suction behaviour is also incorporated. The model has been implemented with a user-friendly interface and runs for the 10 m depth case studies (with 10 cm discretisation) in less than 15 minutes on a 'standard' desktop computer, therefore could be easily incorporated into design practice.

A number of theoretical case studies have been examined which leads to the following conclusions. Self-weight consolidation, in highly compressible materials with properties similar to those examined, provides the majority of the consolidation behaviour. Additional evaporative drying, when the evaporative flux is higher than that of consolidation can lead to substantially denser and therefore stronger materials. Such materials can be considered over-consolidated. If regulation or risk/liability assessments require a strength over that of simply normally-consolidated materials then evaporative drying can yield such materials. If the deposition can be tuned in such a way so that self-weight consolidation takes place when evaporation potential is low, ie during the winter half of the year, then evaporation

potential can be used to further consolidate prior to the next deposition. This means that the layer thickness should be calibrated to enable self-weight consolidation to be to a high percentage complete, and so that the required depth of the layer can be further reduced in water content over the summer half of the year. Water redistribution within these layers can then take place over longer periods of time, leading to a more homogenous material, but one that is over-consolidated and therefore stronger.

ACKNOWLEDGEMENTS

Funding for the development of the model by Shell Canada is gratefully acknowledged.

REFERENCES

- Caldwell, J, Revington, A, McPhail, G and Charlebois, L, 2014. Optimised seasonal deposition for successful management of treated mature fine tailings, in *Proceedings Paste 2014*, pp 371–380 (Infomine: Vancouver).
- Fredlund, MD, Wilson, G W and Fredlund, D G, 2002. Representation and estimation of the shrinkage curve, in *Proceedings Third International Conference on Unsaturated Soils (UNSAT 2002)*, pp 145–149 (Swets & Zeitlinger: Lisse).
- Kim, D J, Diels, J and Feyen, J, 1992. Water movement associated with overburden potential in a shrinkage marine clay soil, *Journal of Hydrology*, 133:179–200.
- Nijssen, T, 2013. Modelling of cyclic drying/re-wetting behaviour of Albian oil sand tailings, MSc thesis, Delft University of Technology, Delft.
- Rijniersce, K, 1983. *A simulation model for physical soil ripening in the IJsselmeerpolders*, Rijksdienst IJsselmeerpolders.
- Romero, E and Vaunat, J, 2000. Retention curves of deformable clays, *Experimental Evidence and Theoretical Approaches in Unsaturated soils* (eds: A Tarantino and C Mancuso), pp 91–106 (Balkema: Rotterdam).
- Seneviratne, N, Fahey, M, Newson, T A and Fujiyasu, Y, 1996. Numerical modeling of consolidation and evaporation of slurried mine tailings, *International Journal for Numerical and Analytical Methods in Geomechanics*, 20(9):647–671.
- Shampine, L F and Thompson, S, 2001. Solving DDEs in Matlab, *Applied Numerical Mathematics*, 37:441–458.
- Shell, 2012. Oil sands performance report 2011 [online]. Available from: <<http://s07.static-shell.com/content/dam/shell-new/local/country/can/downloads/pdf/aboutshell/our-business/oil-sands/oil-sands-performancereport2011.pdf>>.
- Stark, T D, Choi, H and Schroeder, P R, 2005. Settlement of dredged and contaminated material placement areas. I: theory and use of primary consolidation, secondary consolidation and dewatering of dredged fill, *Journal of Waterway, Port, Coastal and Ocean Engineering*, 131(2):43–51.
- van der Meulen, J, van Tol, F, van Paassen, L and Heimovaara, T, 2012. Numerical modeling of drying and consolidation of fine sediments and tailings, in *Proceedings IOSTC 2012*, pp 399–409 (University of Alberta: Edmonton).
- Vardon, P J, Nijssen, T, Yao, Y and van Tol, A F, 2014. Numerical simulation of fine oil sand tailings drying in test cells, in *Proceedings IOSTC 2014*, pp 59–69 (University of Alberta: Edmonton).
- Wang, C, Harbottle, D, Liu, Q and Xu, Z, 2014. Current state of fine mineral tailings treatment: a critical review on theory and practice, *Minerals Engineering*, 58:113–131.
- Yao, D T C and Znidarcic, D, 1997. *Crust Formation and Desiccation Characteristics for Phosphatic Clays, users' manual for computer program CONDES0*, publication number 04–055–134 (Florida Institute of Phosphate Research).